Predicting the spread of Alzheimer's Disease pathology using brain connectomes from different cognitive stages

Arianna Parada Zambrano
arianna.zambrano.22@ucl.ac.uk
University College London
London, UK

Abstract

Tau pathology in Alzheimer's disease (AD) spreads in a stereotypical pattern that is hypothesized to follow the brain's structural connectivity. This project explores how well connectomes from different cognitive stages can predict the regional spread of tau, using network diffusion and production-spread models. Structural connectomes from the ADNI dataset were analyzed across four cognitive groups: cognitively normal (CN), early mild cognitive impairment (EMCI), late mild cognitive impairment (LMCI), and dementia (DEM). We applied an analysis to assess connectivity changes across groups and implemented three network spreading models: the Network Diffusion Model (NDM), the Fisher-Kolmogorov-Petrovsky-Piscounov (FKPP) model, and the weighted FKPP model incorporating regional amyloid-beta. Results showed that the FKPP and weighted FKPP models consistently outperformed the NDM in predicting tau PET data. Incorporating amyloid-beta improved predictions further, particularly in the entorhinal and medial temporal regions. These findings support the hypothesis that tau spread in AD is both connectivity and amyloid-driven, with potential implications for personalized disease modelling.

1 Introduction

Alzheimer's disease (AD) is the most common cause of dementia, affecting over 55 million people worldwide. AD is characterized by the accumulation of two specific proteins: amyloid-beta and tau. Amyloid-beta affects AD by forming plaques in the brain, while tau causes neurofibrillary tangles. While amyloid-beta is thought to commence the disease pathology, the spread of tau is more closely associated with the clinical symptoms and neurodegeneration observed in AD. Notably, tau spreads across the brain in a stereotypical pattern, which can be visualized and quantified using tau positron emission tomography (PET).

Recent advances suggest that tau propagation is not random but follows the architecture of the brain's structural connectivity, its connectome. Derived from diffusion MRI and tractography, the connectome provides a map of white matter pathways that enable communication between different brain regions. Modelling studies hypothesize that tau spreads neuronally along these pathways.

This project leverages structural connectomes derived from participants at different stages of cognitive impairment, cognitive normal (CN), early mild cognitive impairment (EMCI), late mild (LMCI), to dementia (DEM), to investigate how connectivity influences the spread of tau pathology. Using the Network Spreading Models and Brain Connectivity toolboxes, we aim to simulate the propagation of tau through the brain's connectome and assess which models and connectome states best recapitulate observed patterns of tau accumulation. By doing so, we hope to clarify how disease related changes in brain connectivity impact tau spread, and whether early or late stage connectomes are more predictive of tau pathology. This work not only advances our understanding of AD progression but may also inform future modelling approaches and early intervention strategies.

In recent years, network neuroscience has increasingly emphasized the importance of modeling brain disorders through the lens of connectomics. Alzheimer's disease presents a uniquely network-oriented challenge: the spatial progression of tau appears to trace white matter pathways, while at the same time, regional factors like amyloid-beta deposition modulate pathology locally. This dual dependence on global structure and local vulnerability demands computational models that integrate both. Our study contributes to this emerging direction by comparing mechanistic models across distinct stages of AD, leveraging rich multimodal neuroimaging data from the ADNI project and modern network simulation toolkits.

2 Methods

2.1 Data Preprocessing

Structural connectomes for 168 participants were obtained from the Alzheimer's Disease Neuroimaging Initiative (ADNI), divided into four cognitive groups: cognitively normal (CN), early mild cognitive impairment (EMCI), late mild cognitive impairment (LMCI), and probable Alzheimer's disease (AD), each comprising 42 participants. Each participant's connectome was stored as a symmetric adjacency matrix (CSV), with edge weights representing the number of streamlines estimated from diffusion MRI tractography.

Matrices were loaded and validated against the expected number of regions defined in TauRegionList.csv. Prior to analysis, all connectomes were normalized by their maximum edge weight to allow consistent comparisons across subjects.

Tau PET data, provided in tau_ab+_tau+.csv, contained group-averaged SUVRs for 242 tau-positive participants. Amyloid-beta SUVRs, from 241 participants, were used for advanced modelling with the weighted FKPP model and were provided in amyloid_ab+_tau+.csv.

2.2 Graph Metrics

Graph-theoretical measures were calculated using the Brain Connectivity Toolbox (BCT) in Python. For each individual connectome, key metrics were computed:

Node degree (sum of edge weights per node),

Clustering coefficient (proportion of a node's neighbors that are interconnected),

Global efficiency (average inverse shortest path length across the network),

Rich-club coefficient (density of connections among high-degree nodes).

Statistical comparisons across cognitive groups were performed using Kruskal-Wallis tests followed by post-hoc pairwise comparisons with Dunn's test (scipy.stats and scikit-posthocs). Rich-club coefficients were computed for increasing node degree thresholds to assess topological organization differences across disease stages.

2.3 Network Spreading Models

To simulate the spread of tau pathology, we employed the Network Spreading Models Toolbox, which implements three biologically informed models:

Network Diffusion Model (NDM): models tau spread via linear diffusion along the structural connectome.

FKPP Model: adds a logistic growth term to capture uniform local production of tau.

Weighted FKPP Model: extends the FKPP by allowing the local production rate to vary by region, weighted by amyloid-beta deposition.

Implementation was performed using the provided task_2.ipynb script. Group-averaged connectomes were computed for each cognitive stage and used as substrates for model simulations. Each model's parameters—including epicentre (seed region), time, and, for FKPP, the alpha parameter (relative weight of spread vs. production)—were optimized to minimize the sum of squared error (SSE) between model predictions and observed tau PET values.

Model performance was assessed using:

Pearson correlation (r) between predicted and observed regional tau SUVRs,

Corrected Akaike Information Criterion (AICc) for model comparison.

After running the group-averaged connectomes, we ran the same models on individual, participant level connectomes.

2.4 Visualization

Residuals (predicted minus observed tau SUVRs) were visualized using the Enigma Toolbox in enigma.ipynb. These residuals were projected onto cortical surface templates to assess spatial biases in each model's predictions. Visualization was carried out in an isolated environment due to package conflicts.

2.5 Advanced Tasks

In advanced_tasks.ipynb, we explored the influence of regional amyloid-beta on tau production using the weighted FKPP model. Amyloid-beta SUVRs were used to modulate the local production term, with tau spread simulated across each of the four group-averaged connectomes. Model fit (r values and AICc) was compared with baseline NDM and FKPP models to test whether incorporating amyloid improves prediction.

To validate findings, two types of null models were implemented:

Amyloid-beta permutation tests: Regional amyloid maps were randomly shuffled multiple times, and weighted FKPP models were re-fit to generate a null distribution of model performance.

Connectome rewiring: The best-performing group-averaged connectome was degree- and strength-preserving rewired using BCT algorithms, and the NDM and FKPP models were refit across iterations to evaluate robustness of connectivity-specific effects.

These null models were used to benchmark observed model performance and confirm that improvements were not attributable to random structural features. Permutation tests were run with 1000 iterations to construct robust null distributions. In the rewiring analysis, we preserved both node strength and degree. Model performance was compared using not only Pearson's r but also SSE and AICc, providing a multidimensional assessment of predictive accuracy under null conditions. These tests help isolate the extent to which real connectome structure and amyloid distribution explain tau propagation versus what could emerge from random spatial topology.

3 Results

3.1 Connectome Structure

To visualize how structural connectivity evolves, the strongest unique interregional connections were compared between the CN and DEM groups, as seen in figure 1. In CN subjects, dominant connections were centered in fronto-parietal and visual areas. In contrast, DEM participants showed stronger connections in more posterior and medial regions, such as the precuneus and cerebellum, suggesting altered network hubs in disease.

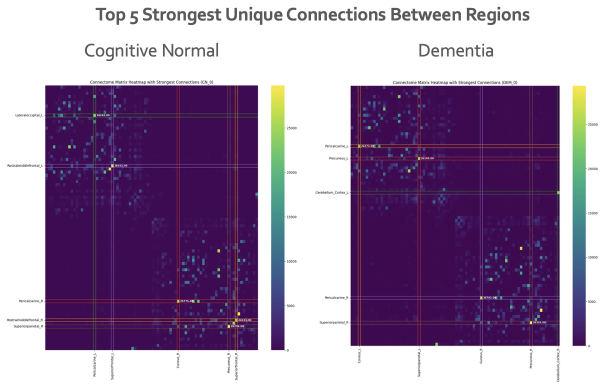

3.2 BCT Connectome Properties

Graph-theoretical analyses revealed statistical differences in structural connectivity across the cognitive continuum from cognitive normal (CN) to dementia (DEM) (Bullmore and Sporns 2009). Clustering coefficient and global efficiency declined with increasing cognitive impairment, indicating disrupted local and global integration of the brain network. A significant group difference in global efficiency was observed ($p < 0.05$). Node degree and rich-club coefficients showed a mild upward trend across groups, with the highest values observed in the DEM group, however no statistical significance was found. Betweenness centrality remained relatively stable, suggesting that hub roles were preserved across progression stages (Yu et al. 2021).

Pairwise comparisons confirmed that the DEM group exhibited significantly reduced global efficiency compared to the CN group. These results support the hypothesis that disease progression disrupts network organization in measurable ways.

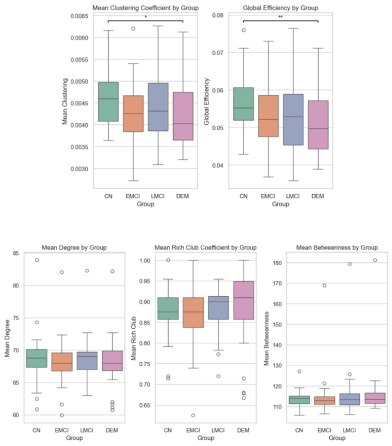

p-value	stars
< 0.05	*
< 0.01	**
< 0.001	***

3.3 NDM vs FKPP

First and foremost we ran, both the NDM model from the network spreading toolbox, as well as the FKPP model. From there we extracted many data points such as, optimal seed, optimal alpha (for FKPP), time point index, SSE, pearson's r value, and the prediction values for each model. From there we were able to use these data points to run a time series script to print the progression of tau as shown by the NDM and FKPP models.

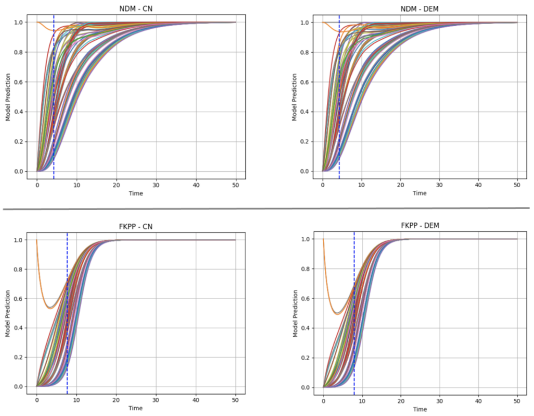

What we observe is that the NDM model remains relatively consistent at the epicenter, while the remaining regions increase. However, when contrasting that to the FKPP model, the epicenter shows a dip in the level of tau before it increases again along with the other regions (Raj et al. 2012; Weickenmeier et al. 2019). This indicates that until the tau reaches the other regions to continue spreading and start replicating, all of the tau is coming from the epicenter and needs to replicate as well.

Using group-averaged connectomes, both the NDM and FKPP models were fit to the tau PET data, and model performance was assessed using squared error, AICc, and AICc weights. Across all four groups (CN, EMCI, LMCI, DEM), the FKPP model consistently outperformed the NDM in terms of lower squared error and better model fit (lower AICc values). AICc weights were >0.8 for FKPP across all groups, indicating high confidence in model selection favoring FKPP. These findings support the inclusion of a local production term in addition to network-mediated spread when modeling tau accumulation.

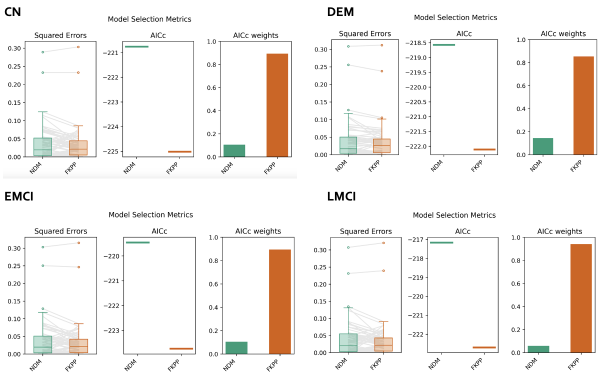

3.4 Enigma Visualization

Upon running the NDM and FKPP models, we were also able to extract the residuals of each model for each cognitive group and save them into a separate .csv file. This allowed us to use the Enigma visualization toolbox to plot the residuals on the cortical surface of the brain. Model residuals, visualized on the cortical surface, revealed consistent spatial patterns of under and overprediction. NDM tended to underpredict tau in temporoparietal and medial temporal regions in DEM patients. FKPP reduced these errors, especially in regions associated with early tau deposition (Goedert 2015). These differences suggest that the FKPP model better captures spatial heterogeneity in tau accumulation.

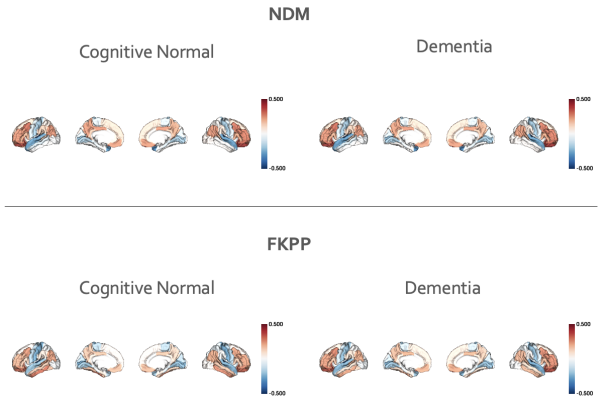

3.5 Individual Level Fitting

To run the individual level fitting, it would cost a lot more computationally than the group-averaged connectomes. Therefore, using the data from the group-averaged connectomes we managed to isolate the top six possible seed regions using the NDM model. This model is quite efficient and does not cost a lot of computation time. What we see from this is that we identify some key patterns in the potential seed regions across different cognitive states. The top regions identified are Inferiortemporal, Temporalpole, Entorhinal, Amygdala, Middletemporal, and Hippocampus.

```
CN Top 5 regions with lowest SSE according NDM

                seed       SSE         r
28  Inferiortemporal  2.478383  0.724249
37      Temporalpole  2.641696  0.618079
14         Entorhinal  2.644907  0.597384
19           Amygdala  2.814673  0.544657
33    Middletemporal  2.900863  0.658039
EMCI Top 5 regions with lowest SSE according NDM

                seed       SSE         r
28  Inferiortemporal  2.519765  0.719243
14         Entorhinal  2.738142  0.580164
37      Temporalpole  2.767463  0.615738
19           Amygdala  2.812019  0.539256
24        Hippocampus  2.903887  0.539922
LMCI Top 5 regions with lowest SSE according NDM

                seed       SSE         r
28  Inferiortemporal  2.622800  0.717790
37      Temporalpole  2.763001  0.608399
19           Amygdala  2.768094  0.548724
14         Entorhinal  2.809329  0.585227
24        Hippocampus  2.967577  0.542361
DEM Top 5 regions with lowest SSE according NDM

                seed       SSE         r
28  Inferiortemporal  2.567709  0.714183
19           Amygdala  2.766200  0.543295
14         Entorhinal  2.855447  0.584053
37      Temporalpole  2.885726  0.609724
24        Hippocampus  2.956375  0.536980
```

Using individual connectomes, distributions of model fit metrics were examined. KDE plots showed a higher average Pearson correlations and lower SSEs for FKPP compared to NDM across all cognitive groups. The epicentre or seed distributions were largely concentrated in the inferior temporal and entorhinal cortex for both models, consistent with known tau pathology onset sites (Vogel et al. 2023). This demonstrates that the FKPP model provides a better fit not only at the group level but also at the individual level, highlighting its robustness across scales.

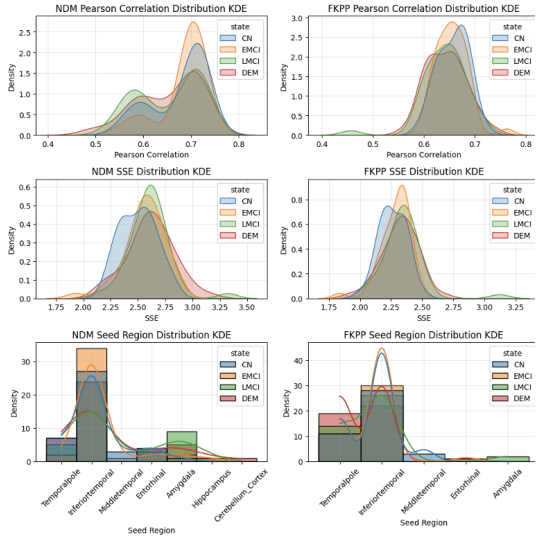

We also analyzed how model-optimized seed regions varied across groups. While early-stage groups (CN, EMCI) showed greater variability in seed localization, later stages (LMCI, DEM) consistently pointed to the entorhinal and inferior temporal cortex. This convergence supports the role of these regions as early hubs of tau propagation, aligning with Braak staging and prior imaging literature (Vogel et al. 2023).

3.6 Weighted FKPP

The weighted FKPP model, similar to the FKPP model, incorporates a logistic regression growth term. However for this particular model, the production of tau is not uniform for each region, but rather it is dependent on the amyloid-beta values for each region. When running this model, we see an interesting change in results, particularly regarding the seed. Before for both the NDM and FKPP models, the seed was printed as Inferiortemporal, yet for the weighted FKPP model the new seed is now Entorhinal (Thompson et al. 2024). The weighted FKPP model, incorporating regional amyloid-beta SUVRs to scale tau production, demonstrated superior fit compared to both NDM and FKPP models across all cognitive stages. Squared errors were further reduced, and AICc weights consistently favored the weighted FKPP model. This improvement supports the hypothesis that amyloid-beta plays a regional, modulatory role in promoting tau pathology beyond what is captured by structural connectivity alone.

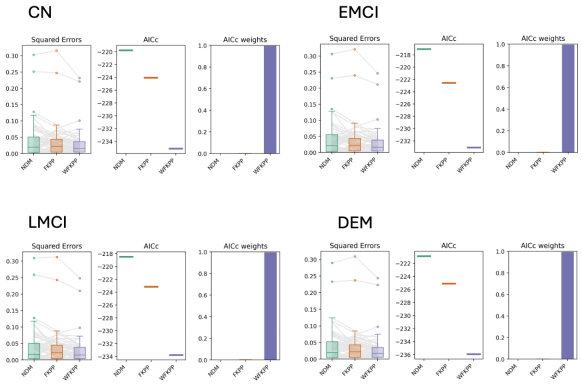


```
{'CN':    Model        AICc  AICc weights  rank
 0    NDM -220.901597      0.000543     3
 1   FKPP -225.096799      0.004424     2
 2  WFKPP -235.928324      0.995033     1,
 'EMCI':    Model         AICc  AICc weights  rank
 0    NDM -219.775570      0.000462     3
 1   FKPP -224.056895      0.003926     2
 2  WFKPP -235.128339      0.995612     1,
 'LMCI':    Model         AICc  AICc weights  rank
 0    NDM -217.050355      0.000326     3
 1   FKPP -222.555668      0.005121     2
 2  WFKPP -233.093618      0.994553     1,
 'DEM':    Model        AICc  AICc weights  rank
 0    NDM -218.493878      0.000475     3
 1   FKPP -223.146266      0.004861     2
 2  WFKPP -233.788513      0.994664     1}
```

Using the weighted FKPP model to extract valuable new information, we run the original FKPP model with some fixed parameters. From the WFKPP model, we gather the optimal seed, alpha, and timepoint to set as parameters in our FKPP model. Furthermore, when we compare the enigma visualization of the WFKPP model to the FKPP model we see that the over and under estimations are very similar for both the cognitive normal and dementia groups. However, the WFKPP model seems to have less intensity of color in some areas informing us that the weighted model matches the best for tau spread.

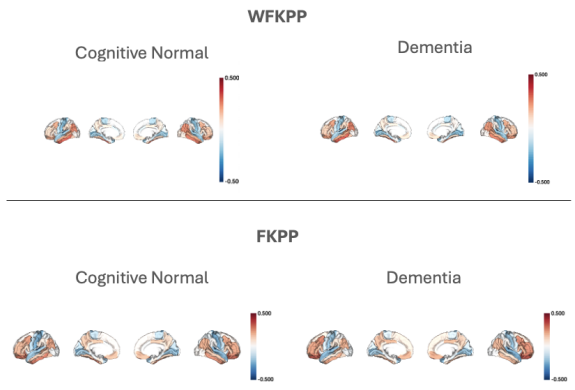

3.7 Null Testing

To confirm biological relevance, we permuted amyloid maps and rewired connectomes using degree-preserving algorithms (Váša and Mišić 2022). In both cases, model performance degraded, verifying that observed improvements in FKPP and weighted FKPP were not due to chance.

4 Discussion

Our study demonstrates that tau pathology in AD is better modeled by incorporating both network-mediated spread and regionally variable production mechanisms. The FKPP model, which adds a local logistic growth term to the traditional NDM, consistently outperformed NDM at both group and individual levels. This confirms that passive diffusion alone cannot explain the spatial pattern of tau accumulation (Raj et al. 2012).

Further, our weighted FKPP model, which uses amyloid-beta deposition to modulate local tau production, provided the best overall fit. This result aligns with mechanistic findings that amyloid-beta acts upstream to facilitate tau misfolding and aggregation (Goedert 2015; Thompson et al. 2024). The shift of the seed region from inferior temporal (NDM, FKPP) to entorhinal cortex (weighted FKPP) further supports a more biologically realistic model of disease initiation.

At the network level, our analysis confirmed a loss of integration (via reduced global efficiency) with preserved core hub roles, in line with prior connectome studies of AD (Yu et al. 2021). Importantly, our null model analysis reinforces the robustness of our results, ruling out artifacts from topological or statistical noise (Váša and Mišić 2022).

Our results contribute to the growing body of literature advocating for precision models of neurodegeneration that account for inter-individual differences in network topology and molecular burden. Clinically, these models could support early diagnosis by identifying likely epicentres based on connectome structure, or inform targeted therapeutic strategies that disrupt tau spread pathways.

4.1 Limitations and Future Directions

Group-averaged connectomes, while convenient, may obscure individual variability. Future work should explore longitudinal modeling with personalized connectomes and integrate functional connectivity or genetic risk factors. The success of amyloid-weighted models also invites multimodal strategies that jointly model both amyloid and tau PET with structural data.

Additionally, the static nature of the connectomes used (derived from a single diffusion scan) limits our ability to account for time-varying changes in brain structure. Incorporating longitudinal diffusion data could better reflect the evolving substrate on which tau spreads. Finally, exploring functional connectivity alongside structural networks may reveal synergistic or dissociative patterns of vulnerability, especially in early disease.

In conclusion, this work strengthens the case for mechanistic, connectivity-based models of AD pathology and highlights the value of integrating multimodal biomarkers for more accurate and biologically faithful disease prediction.

5 References

1. Goedert M. Alzheimer's and Parkinson's diseases: The prion concept in relation to assembled AB, tau, and a-synuclein. Science (1979). 2015;349(6248). doi:10.1126/science.1255555 2. Vogel JW, Corriveau-Lecavalier N, Franzmeier N, et al. Connectome-based modelling of neurodegenerative diseases: towards precision medicine and mechanistic insight. Nat Rev Neurosci. 2023;24(10):620-639. doi:10.1038/s41583-023-00731-8 3. Yu M, Sporns O, Saykin AJ. The human connectome in Alzheimer disease — relationship to biomarkers and genetics. Nat Rev Neurol. 2021;17(9):545-563. doi:10.1038/s41582-021-00529-1 4. Thompson E, Schroder A, He T, et al. Demonstration of an open-source toolbox for network spreading models: regional amyloid burden promotes tau production in Alzheimer's disease. Alzheimer's & Dementia. 2024;20(S9). doi:10.1002/alz.093791 5. Raj A, Kuceyeski A, Weiner M. A Network Dieusion Model of Disease Progression in Dementia. Neuron. 2012;73(6):1204-1215. doi:10.1016/j.neuron.2011.12.040 6. Weickenmeier J, Jucker M, Goriely A, Kuhl E. A physics-based model explains the prion-like features of neurodegeneration in Alzheimer's disease, Parkinson's disease, and amyotrophic lateral sclerosis. J Mech Phys Solids. 2019;124:264- 281. doi:10.1016/j.jmps.2018.10.013 7. He T, Thompson E, Schroder A, et al. A Coupled-Mechanisms Modelling Framework for Neurodegeneration. In: Greenspan H, Madabhushi A, Mousavi P, et al., eds. Medical Image Computing and Computer Assisted Intervention – MICCAI 2023. Springer Nature Switzerland; 2023:459-469. 8. Oxtoby NP, Garbarino S, Firth NC, Warren JD, Schott JM, Alexander DC. Data- Driven Sequence of Changes to Anatomical Brain Connectivity in Sporadic Alzheimer's Disease. Front Neurol. 2017;8. doi:10.3389/fneur.2017.00580 9. Bullmore E, Sporns O. Complex brain networks: graph theoretical analysis of structural and functional systems. Nat Rev Neurosci. 2009;10(3):186-198. doi:10.1038/nrn2575 10. Thompson E, Schroder A, He T, et al. Combining multimodal connectivity information improves modelling of pathology spread in Alzheimer's disease. Imaging Neuroscience. 2024;2:1-19. doi:10.1162/imag_a_00089 11. Váša F, Mišić B. Null models in network neuroscience. Nat Rev Neurosci. 2022;23(8):493-504. doi:10.1038/s41583-022-00601-9